Research Article

Journal of Chemistry Letters
journal homepage: www.jchemlett.com
ISSN (online) 2717-1892 (print) 2821-0123

Comparative studies on quartz surface charge and brine ions interaction for oil detachment by sessile drop method and molecular dynamics simulation

Ernest Peter MAIKI[1, *], Renyuan SUN[1, *], Yingsong HUANG[2], Shaoran REN[1]

[1.]*School of Petroleum Engineering, China University of Petroleum (East China), Qingdao, China*

[2.]*Petroleum Exploration and Development Institute, Shengli Oilfield Company, Sinopec, Dongying, Shandong, China*

ARTICLE INFO

Article history:
Received
Received in revised form
Accepted
Available online

Keywords:
Total disjoining pressure
brine -Rock interaction
sessile drop
Molecular dynamics simulation
surface active components

ABSTRACT

low salinity-surfactant brine on hydrophobic quartz surface for wettability alteration to mimic multiphase fluids flow in porous media was investigated using sessile drop experiments and molecular dynamics (MD) simulation. The surface-active components in crude oil shifted towards the oil-water interface leading to a reduction in interfacial tension γ_{ow} and consequent reduction in contact angles for low brine concentrations. Further decreased brine concentrations resulted in dissolution of surface-active components into bulk brine. However, with increased brine concentrations, negative sites were induced on the quartz surface and boosted the adsorption of Ca^{2+} ions. The adsorbed cations bridged with the polar compounds in the crude oil resulting in the adherence of the organic molecules on the quartz surface. The monitoring and measurement of contact angles by sessile drop experiment was done. The initial and final contact angle readings were taken in ranges (77^o-51^o) to (18^o- 05^o) for NaCl brine while for CaCl2 brine, contact angles in ranges (70^o-60^o) to (19^o - 06^o). Intermolecular forces were found to play a key role, which resulted in electrostatic molecular attractions and oil shift from the surface as shown by relative concentration measurements in molecular dynamics simulation. Sodium chloride and Calcium chloride brines of varying concentrations (2,000 mg/L-50,000 mg/L) and sodium dodecyl sulfate (250 mg/L) as a surface-active agent was used.
.

1. Introduction

The presence of hydrophilic and hydrophobic interfaces are ubiquitous in nature and are of great scientific importance for research and industrial applications[1]. Numerous investigations have been done to characterise brine-oil interfaces and understand the physiochemical interactions between accompanying fluids and rock surfaces. These have provided important milestone for understanding complex crude-oil-brine interactions and reservoir lithology for tertiary extraction of oil by low salinity water flooding (LSWF)[2]–[4]. The low salinity effect and its mechanisms despite a plethora of research spanning for decades, is still elusive except wettability alteration which is generally agreed upon by many scholars[5]–[8]. Studies on fluid-fluid and fluid-rock interaction with interfacial tensions (IFT) are very important in understanding multiphase flow in porous media and its herein highlighted in this manuscript.
The brine ions contribution together with surfactants at the oil-brine interface is found to play a critical role and thus needed to be understood at atomistic and higher-level scales[9]. The charged group species for both rock surface and brine are reported to contribute to the hydration repulsion force which have effects on both ionic strength and cation valance[10]. This ionic contribution at oil-brine and rock interfaces was studied and tackled on a multi-scale approach from atomistic to sub pore level scale by many authors[11]–[15].This has provided an importance basis for evaluating the role of brine ions and there contribution in removing adsorbed crude oil on rock surfaces.
Molecular dynamics (MD)simulations help to understand better the particles flow paradigm at both pore and core levels [16], [16]–[18]. MD simulations provide insights that help in explaining theories which are developed for improving the existing models for surface fluids flow and their intermolecular interactions. Underwood et al. studied salinity dependence of interfacial tension for decane in contact with aqueous NaCl solutions, they

∗ Corresponding author. e-mail: epmaiki@cns.mak.ac.ug or epmaiki@yahoo.com

observed that boundary layer thickness decreases upon increasing salinity, resulting in higher IFTs [19], while Zhao et al. expanded that work by focusing on diluted NaCl solutions and observed a nonmonotonic trend of IFT for n-decane/brine systems which is helpful in oil removal[20]. Remesal et al. considered IFT values of aqueous brine(NaCl, CaCl2) and oil (dodecane, benzene) and found out that calcium ions were more surface-active than sodium ions, due to the larger hydration shell compared to sodium [21]. Currently, the main focus is on the surface behavior of polar and heavy compounds of crude oil, which attempt to reveal the effects of salinity on the oil-brine interfaces. The effect of surface charge density on low salinity ions and their interaction with non-polar hydrocarbons via brine-oil interface is emphasized. Consequently, interfacial tension behavior for brines; NaCl and CaCl2 with sodium dodecyl sulfate (SDS) needed to be studied. Nezhad et al. Studied effects interfacial tension using different brine solutions: Na2SO4, CaCl2, MgSO4, KCl, CaSO4, NaCl, MgCl2 and crude oil, they observed that brine ions changed interfacial tension and contact angles with respect to acidic crude oil [22].

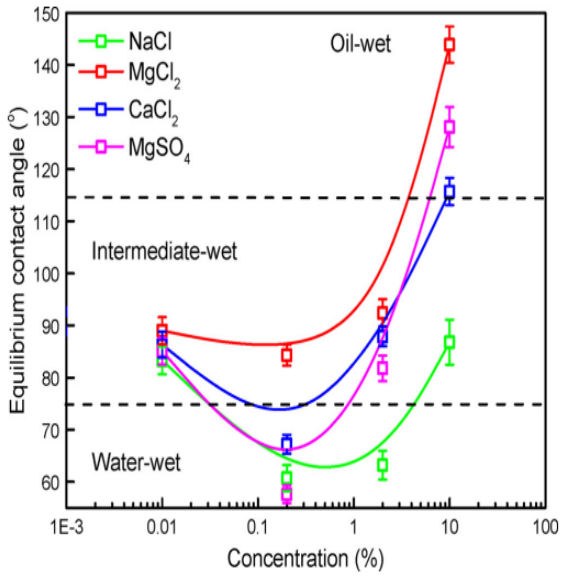

Figure 1. Contact angles measured on flat quartz slides[23]

Despite these kinds of research done, the mechanisms for low salinity water effect (LSWE) remain at large with further explanations needed. Originally, reservoir rocks were water-wet but turned to oil-wet due to the deposition/adsorption of several indigenous organic polar species of asphaltenes, resins and naphthenic acids in crude oil[24]–[26]. To mimic this, quartz slides were aged in oil to establish an oil wet state before low salinity -surfactant studies.

Wei eta al (2018) showed that different ion types had unique impacts on the measurement results of wetting angles and the affinity of quartz surface for brine ions interaction was according to this trend NaCl > MgSO4 > CaCl2 > MgCl2 as shown in Figure 1. Based on this, NaCl and CaCl2 were chosen for low salinity- surfactant highbred sessile drop and MD simulation studies.

1.1 Chemical description of quartz and the negative charge origin on the surface

Quartz is the main component of sandstone, so quartz slides will be used to replace sandstone in this manuscript[27]. The Quartz is comprised of Si–O–Si linkage structures with hydrophilic hydroxyl surface group terminations [28]. The Silanol groups on silica surface are formed via two

main processes. (1) During condensation polymerization when silica is synthesized from Si $(OH)_4$ to form the xerogel. The supersaturated solution of the acid is converted into a polymer and this happens by changing spherical colloidal particles into SiOH groups on the surface. (2) The surface OH groups can also form as a result of rehydroxylation of dehydroxylated silica by addition of water or aqueous solutions. It's this adsorbent property that makes amorphous silica surface unique in research and engineering applications.

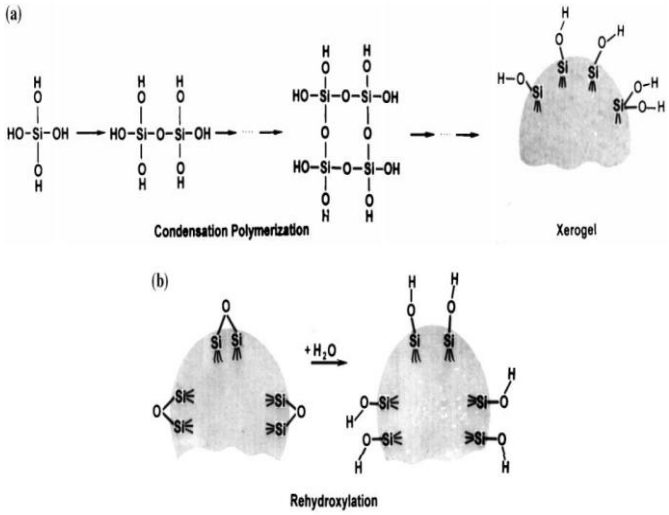

Figure 2. The formation of silanol groups on the silica surface: (a) Condensation polymerization; (b) Rehydroxylation[29]

1.2 Quartz interaction with Hydroxyl and hydronium ions

Surface silanol groups (–Si–OH) interact with hydroxyl (OH^-) or hydronium (H^+) ions from water through two processes: Protons are adsorbed on Si–OH surface under acidic conditions to form a positively charged surface while under alkali pH conditions, the surface of Si–OH deprotonates to form a negatively charged surface as shown below.

$$\equiv Si{-}OH + H_3O^+ \leftrightarrow \equiv Si{-}OH_2^+ + H_2O$$

$$\equiv Si{-}OH + OH^- \leftrightarrow \equiv Si{-}O^- + H_2O \quad (1)$$

where $\equiv SiOH_2^+, SiOH, and \equiv SiO^-$ represent the protonated, neutral, and deprotonated surface sites. The

presence of more than one type of surface species implies that there can be multiple reaction mechanisms occurring on the quartz surface during dissolution. However, the overall reactivity of the quartz surface depends on the relative distribution of the three species[28], [30].

1.3 The surface charge density and its kinetics on quartz

The chemistry of quartz surface and the origin of negative charge is very important in physical and chemical interactions of quartz with hydrophilic and hydrophobic molecules at all length scales for research and field engineering applications. This is the property which dictates the applicability of quartz material for surface wettability studies. The extend of adhesion and cohesion forces between the fluids of interest and the quartz surface depend on the surface charge density and fluids in contact[31]. The creation of negative charges is initiated by de-protonation of silanol groups (≡Si-OH) on the surface of silica through a series of steps illustrated below:

$-SiOH \square \quad -SiO^- + H_S^+$ The amount of all the silanol groups per surface area, Γ_T (1 / m2) is

$\Gamma_T = \Gamma_{SiOH} + \Gamma_{SiO^-}$ where Γ_{SiOH} is the amount of –SiOH per surface area and Γ_{SiO-} is the amount of SiO^- per surface area. The surface charge density, σ (C/m2), is $\sigma = e\Gamma_{SiO^-}$ and e is the elementary charge. According to the law mass action:

$\frac{a_{H^+}^s \Gamma_{SiO^-}}{\Gamma_{SiOH}} = K = 10^{-P^K}$ where K or 10^{-pK} is the dissociation constant and a_{H^+} (mol L^{-1}) is the activity of protons adjacent to the surface.

$a_{H^+}^S = a_{H^+} \exp\left(\frac{-e\Psi_o}{k_B T}\right)$ where a_{H^+} is the activity of proton in bulk solution, Ψ_0 (V) is the surface potential, k_B is the Boltzmann constant and T is the absolute temperature. The surface charge density is given by the following equations:

$$\sigma = C_s(\Psi_o - \Psi_d)$$

$$\sigma = -\sigma_d = \left(\frac{2\varepsilon k K_B T}{e}\right)\sinh\left(\frac{e\Psi_d}{2K_B T}\right) \quad (2)$$

C_S (F/m2) is the Stern layer capacitance, Ψ_d is the potential at the outer surface of the Stern layer (the diffuse layer potential), ε (F/m) is the permittivity of the solvent (water), κ (/m) is the Debye–Hückel parameter and σ_d (C/m2) is the charge density in the diffuse layer[29], [31], [32].

1.4 Effect of PH on surface charge

Zhuravlev in 2000, carried out experiments on adsorption of SDS and showed that its adsorption increased with decrease in pH. When the pH increases, protons in silanol groups, ≡Si-OH, are released from the surface and the negative charges increase, which automatically increases the charge density. The adsorption of SDS becomes larger when the adsorption site potential becomes larger, since SDS is negatively charged, the magnitude of the negative potential near the silica surface will increase with the increase of pH and the electrostatic repulsive force between SDS and the silica increases, which eventually decreases the adsorption rate. This property makes SDS a good candidate for low brine-surfactant hybrid studies.

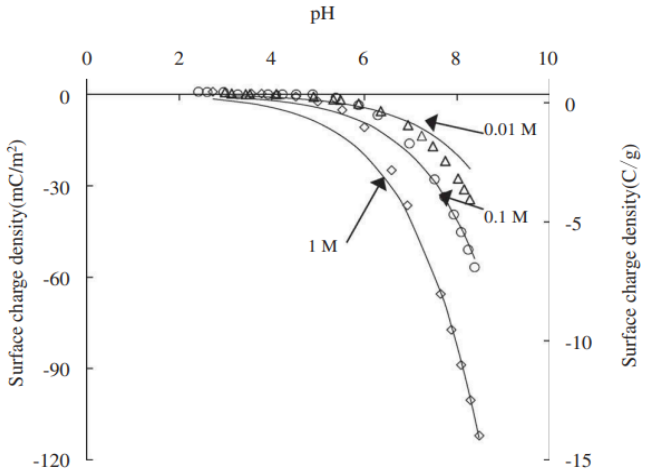

Figure 3. shows relationship between pH and surface charge density on a hydrated quartz surface[33]

1.5 Ionic brine interaction with the Quartz surface and total disjoining pressure

Studies have shown that, three main interactions are possible when polar components of crude oil are on rock surfaces, where acid - base and ion binding interactions occur [24], [26], [34], [35]. Due to these interactions, polar molecules are adsorbed on silicate rock surface by van der Waals forces or hydrogen bonding (Negative disjoining pressure). There by altering the hydrophilic original rock surface state to oil-wet [36]. Furthermore, the negatively charged acidic components cannot be adsorbed onto the equally negatively charged silicate rock because of electrostatic repulsion (positive disjoining pressure) which is helpful for oil recovery. The effect of brine concentration on disjoining pressure at distances less than ~14 nm was reported by Tangparitkul et al. where the disjoining pressure decreasing with increasing brine concentration[37]. However in overall, the disjoining pressure profiles for CaCl2 differed to that of measured NaCl whose profile showed strongly negative disjoining pressures over long-range separation distances above 20 nm and becoming more increasingly attractive with increasing CaCl2 concentration [37]. The high-valent cations are found to bind the acidic components and rock surfaces via ion-binding interactions, taking advantage of the negatively charged rock surface exhibited by most sandstone rocks [5], [38], [39]. The increase in brine concentration of NaCl and

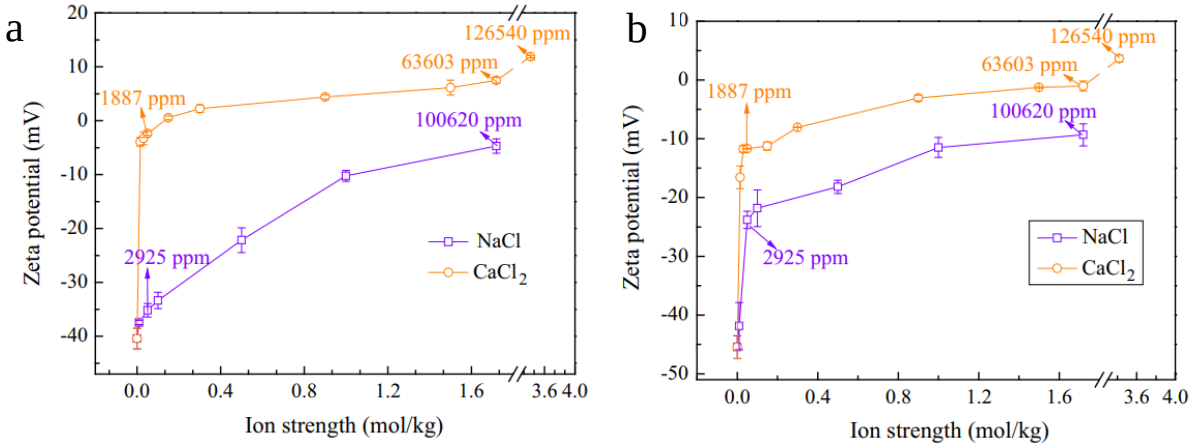

Figure 4. (a) Zeta potential of rock/brine interface while (b) Zeta potential of oil/brine interface at 318K[40]

CaCl2 resulted in a decrease in negative zeta potentials for quartz/brine and oil/ brine interfaces as reported by Hua et al below.

The highest negative charges were observed with rock/ deionized water and oil/deionized water interfaces due to dissociation of silanol groups on rock surface and carboxyl groups in oil. Increasing salinity of NaCl solution resulted in compression of the electrical double layer which decreased negative charges of two interfaces. With Calcium ions, the effect of charge on two interfaces were more strongly than that of Na^+ at the same ionic strength, weak positive charge at rock/brine interface and weak negative charge at oil/brine interface were observed at 63,603 ppm CaCl2 solution. These results suggest that the ion composition and salinity are very important in determining the interactions between the rock/brine and oil/brine interfaces because they can strongly affect the electrical charge at both interfaces[40]. The influence of adhesion and cohesion forces on solid -liquid interface was highlighted [41]–[43]. Oil−brine−rock systems, where brine films are confined between rocks and oil droplets are found to depend on the characteristics of the rock surface, brine composition and chemical properties of the oil droplets [44]. It is with in the interest of this work to: (1) understand low salinity-surfactant ions interaction with the charged quartz surface. (2) study low salinity brine- surfactant hybrid interaction with hydrophobic quartz surface at atomistic level and sub pore. This will relate contact angle variation trend with molecular dynamic simulation of low salinity brine-surfactant on hydrophobic surface.

1.7 Molecular dynamics (MD) simulations

Molecular dynamics (MD) simulation of low salinity-surfactant brine on a hydrophobic quartz surface was studied to gain an insight on molecular motion. The molecular simulations of brine-crude oil- rock systems have been reported to have effects on wettability due to dynamic adsorption of active components on the rock surface rendering it oil wet [45]–[47]. Mabudi et al.(2019) argued that increasing brine ionic concentrations in the presence of n-decane is linked to a decrease in free energies and an increase in the wetting state of a sandstone[48]. Similar work was done by Jia et al.(2019) where oil-wet quartz surface became more water-wet upon removing adsorbed crude oil molecules using mixed surfactant and used contact angle measurements to ascertain the effect in wettability alteration[49]. This was by mixing different surfactants to reduce interfacial tension.

2. Experimental section

2.1. Materials

Chemicals sodium chloride (NaCl > 99.5 wt%), calcium chloride anhydrous (CaCl2, 99.99%) were purchased from Aladdin Chemical Reagent Company. All the chemicals where of analytical grade were used as received. Deionized water was used in all the experiments. The crude oil was obtained from the Shengli oilfield with viscosity 22,500 mPa at 60°C

Table 1. crude oil Composition

Components	Percentage (%)
Aromatic hydrocarbons	31.13
Saturated Hydrocarbons	36.12
Resins	22.42
Asphaltenes	10.33

Table 2. Brine Compositions of ions (mg/L)

No	Na^+ (mg/L)	Ca^{2+} (mg/L)	SDS (mg/L)	Total Salinity(mg/L)
1	49,750	49,750	250	50,000
2	29,750	29,750	250	30,000
3	9750	9750	250	10,000
4	4750	4750	250	5,000
5	1750	1750	250	2,000

2.2 Procedure

contact angle variation by sessile drop experiment with varying low salinity-surfactant concentrations (2) Molecular dynamics simulation to study the dynamic displacement of dodecane oil from quartz surface using optimum 6.1%wt brine.

2.2.1 Contact angle measurements of by sessile drop method

The cleaned quartz slides were immersed in crude oil of known composition and allowed to age for 7 days and left to stand outside for 3 days at room temperature. low salinity-surfactant brines were prepared as shown in table 2 above with 250mg/l Sodium dodecyl sulphate. Droplets of about 1 µL were dripped on quartz surface using a micro injector syringe to study their effects on wettability alteration by periodic changes in contact angles. The images of the droplets were taken with a camera as shown below and the contact angles measured. These measurements were all done at room temperature (25 °C) and pressure (1 atm).

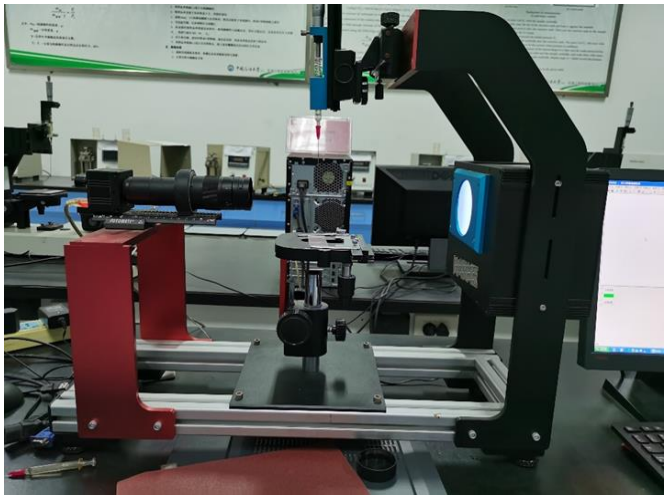

Figure 5. HARKE-SPCA Contact angle tester for angle measurements

2.2.2 Molecular dynamic simulation to study oil removal by low salinity water

Molecular dynamics simulations were conducted by using Materials Studio 8.0 software package. All the simulations were carried out under the COMPASS force field under the NVT ensemble at 300 K. The α-quartz surface used was of dimension 4.85 × 4.39 × 1.6 nm^3, perpendicular to the z-axis from the surface. The silica surface generated was cleaved to α-quartz along the (001) crystallographic orientation and hydroxylated using hydroxyl with density of 7.64nm^{-2} to demonstrate water-saturated rock. This was consistent with crystal chemistry calculations of 5.9–18.8nm^{-2} [50]. The amorphous cell was then constructed of 120 dodecane molecules geometrically optimised and combined with optimised silica surface to form an adsorbed oil-quartz surface. Amorphous brine cells were constructed of varying salt molecules for both NaCl and $CaCl_2$ i.e, 0, 34, 1194, 2000 and 2800 molecules. To each of the 4 brine cells containing brine molecules, was added 10 molecules of sodium dodecyl sulphate (SDS) and topped up with water molecules to a total of 4000 in a cell. These cells built were all geometrically optimised and relaxed by 1 ns NPT MD simulation at 300 K and 1 atm. Each low salinity - surfactant cell was combined with oil-quartz surface and vacuum slab added to eliminate the effect of periodic boundary condition and geometrically optimized. All low salinity-surfactant cells underwent, 2ns NPT MD simulation to remove bad contact between water and brine molecules.

Then a 50ns NVT MD simulation was performed for every built slab at 300 K with the silica surface being fixed in all calculations with a cut off of 12.5Å and a time step of 1fs. Periodic boundary conditions were applied in all three dimensions. All the atoms, cells and quartz surface cells were all optimized using the steepest descent method and 10ns equilibrium molecular dynamics simulation to obtain equilibrium adsorption configuration under NVT ensemble. The results were analysed based on relative concentration which was used by many scholars[51], [52].

2.2.3 Low salinity brine ions of NaCl and CaCl2 interaction with dodecane (modal oil) on a quartz surface by molecular simulation

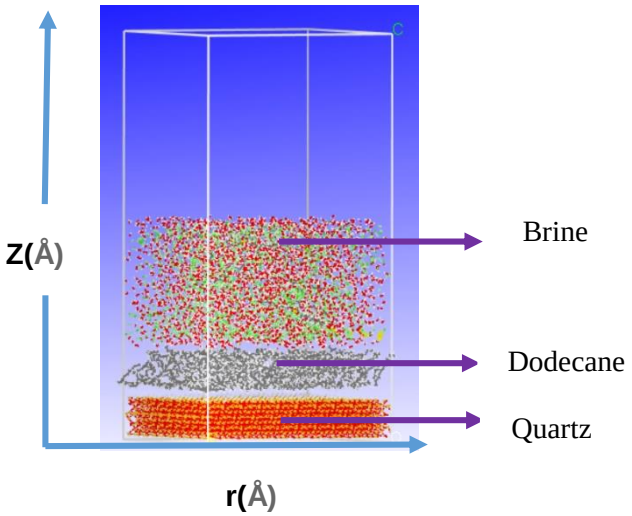

Figure 6. Shows snap shots of optimum low salinity brine of 6.1wt% (NaCl+SDS) interaction with model oil dodecane adsorbed on the quartz surface by molecular dynamic (MD) simulation

3. Result and discussions

3.1 Graphical representations of rate of change of contact angles for NaCl and CaCl2 with varying ionic concentrations. The static contact angles formed by brine droplets on a hydrophobic quartz surface can be given by the Young's equation (1) below.

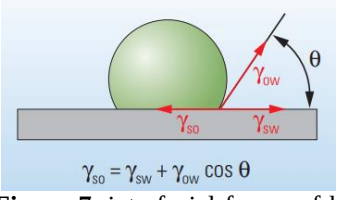

$$\cos\theta = \frac{\gamma_{ws} - \gamma_{so}}{\gamma_{ow}}$$

Figure 7. interfacial forces of brine-oil, brine-quartz and oil-quartz

This equation demonstrates three interfacial forces balance between brine-crude oil (γ_{ow}), brine-quartz (γ_{ws}),

and crude oil-quartz (γ_{so}). The increase in γ_{ws} and γ_{ow} will cause an increased surface water-wetting state, while the increase in γ_{so} and will oppose it. With regard to the brine-crude oil interface, the distribution and orientation of polar compounds interfere with the presence of cations in the brine. The decrease in the salt concentration, resulted in the movement of sodium dodecyl sulfate ion towards the oil-water interface leading to a reduction in interfacial tension and caused reduction in contact angles as shown above. While further decrease causes dissolution of these surface-active compounds into bulk brine.

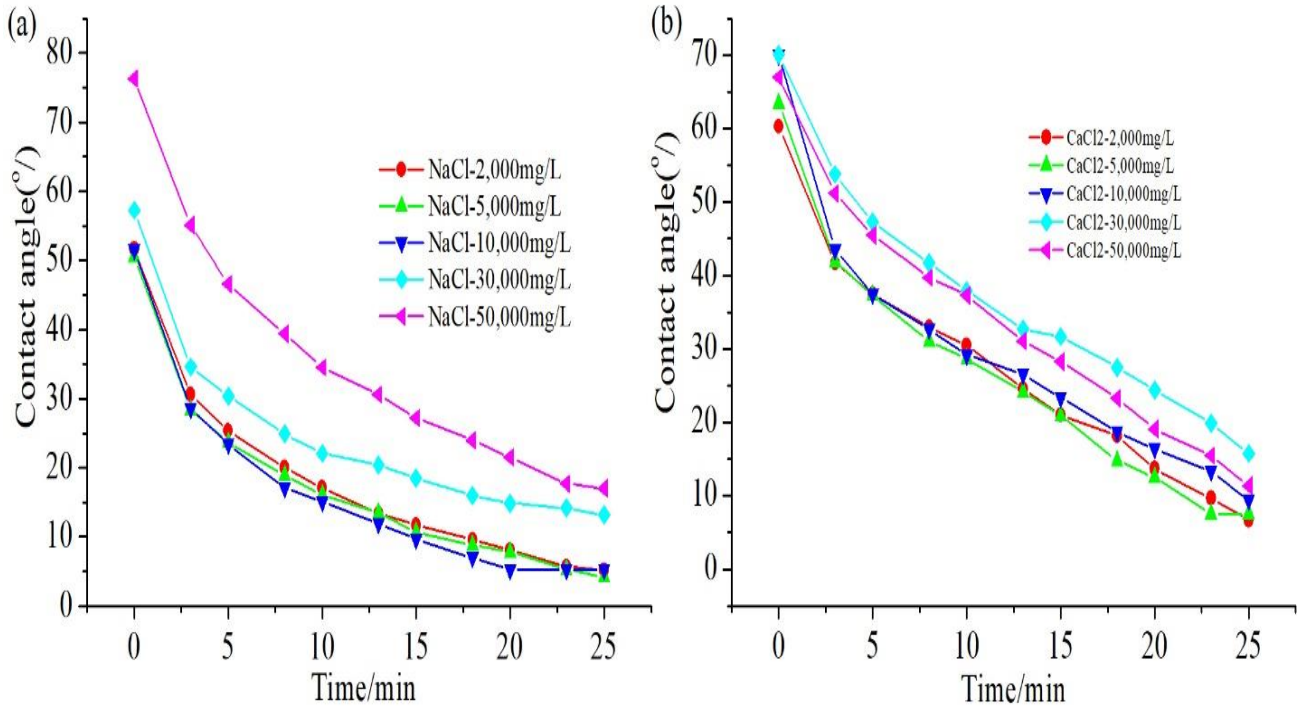

Figure 8. Contact angles of variable concentrations of brine: Graphs (a) Sodium chloride and (b) Calcium Chloride respectively

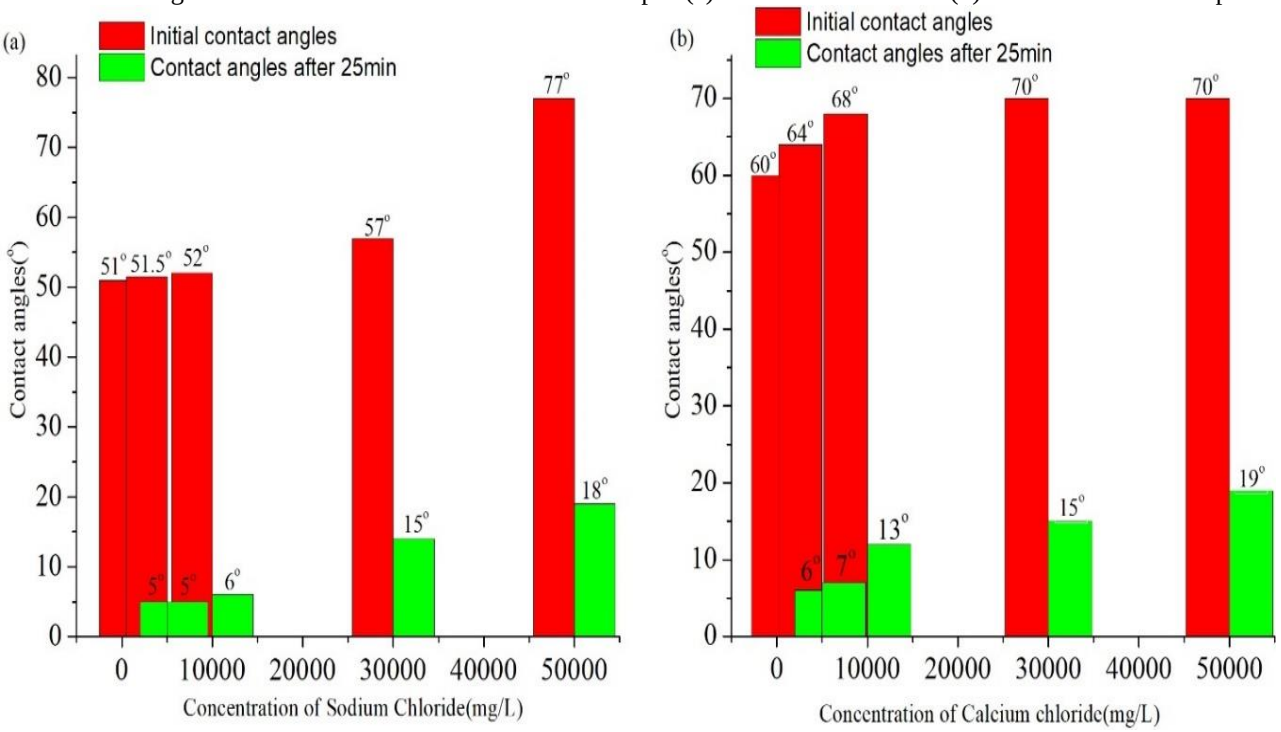

Figure 9. shows Histograms of Initial and final Contact angles of variable brine concentrations: (a) Sodium chloride and (b) Calcium Chloride

The higher initial contact angles resulted in a remarkable decrease in contact angles after 25minutes for both NaCl and CaCl2.

3.2 The effect of contact angles with concentration for NaCl and CaCl2

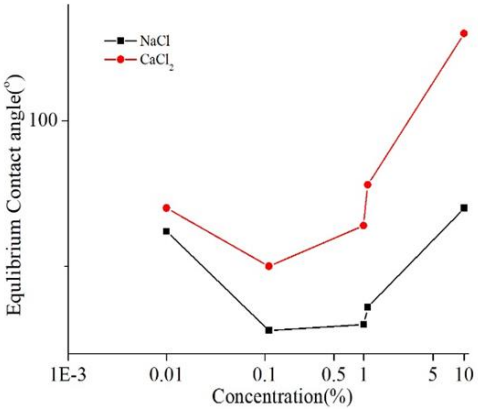

Fig 10. Contact angles NaCl and CaCl2

In **Figure 9**. above, the initial state of the contact angles at ultra-low salt concentrations were 81° and 85° for NaCl and CaCl2 respectively. The wettability of quartz surface lie in an intermediate water-wet state. However, with increased salt concentration, the contact angles declined to almost stand still, with increased concentrations as shown in Fig 10. This suggested the turning of quartz surface to an oil wet state at higher salt concentrations. Wei et al. (2018) considered four salts brines of NaCl, MgSO4, MgCl2 and CaCl2. In there studies, they found that quartz surfaces had varying affinities for cations according to the order NaCl > MgSO4 > CaCl2 > MgCl2 [23]. It was reasoned that divalent cations Ca^{2+}, Mg^{2+} at high concentrations of brine induced creation of negative charges on the quartz surface and these resulted in their adsorption. This resulted in bridging with polar compounds in the crude oil and quartz surface through electrostatic effect leading to adherence of the organic species on the surface. This eventually results in increased contact angles and increased oil-wetting state of quartz surface. For further explanation, we consider the Ionic strength and brine double layer Equations (4&5) below respectively.

$$I = \frac{1}{2}\sum_j C_j Z_J^2 \tag{4}$$

where C is the molar concentration (mol/L) and z is the valence of ions. At low concentration (< 0.1 M), the thickness of the double layer (as measured by the Debye length) is related to the ionic strength of an electrolyte.

$$\lambda = \left(\frac{\varepsilon K_B T}{1000 N_A e^2 I}\right)^{\frac{1}{2}} \tag{5}$$

where k_B is Boltzmann's constant (J/K), T is temperature (K), ε is the permittivity of vacuum (F/m), N_A is Avogadro's number (mol^{-1}), and e is the charge on an electron. From the above two equations, the relationship between brine thickness and ionic charge can be drawn. The thickness of an electrical double layer λ is inversely proportional to the ionic strength I and the decrease of ion strength is expected to produce a more water-wet surface. This is in line with double layer expansion (DLE), suggesting a decrease in contact angle.

3.3 Relative concentration analysis of low salinity ions NaCl and CaCl2 interaction with dodecane on quartz surface by molecular simulation

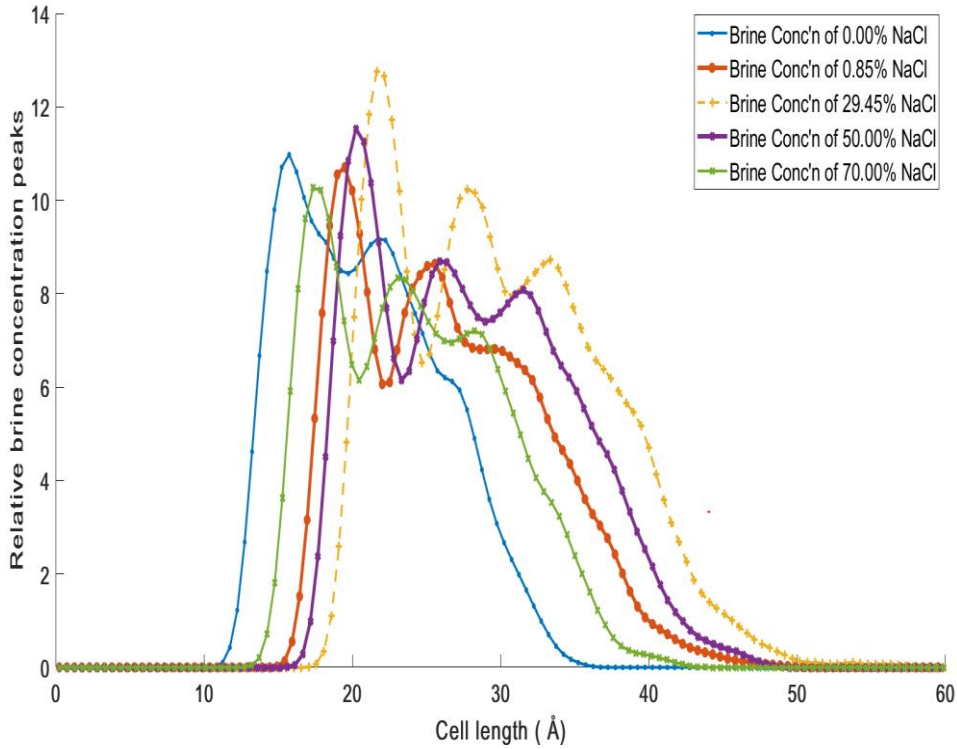

Figure 11. Shows snap shots of oil and NaCl brine relative concentrations graphs on quartz surface @ 300K by molecular dynamic (MD) simulation

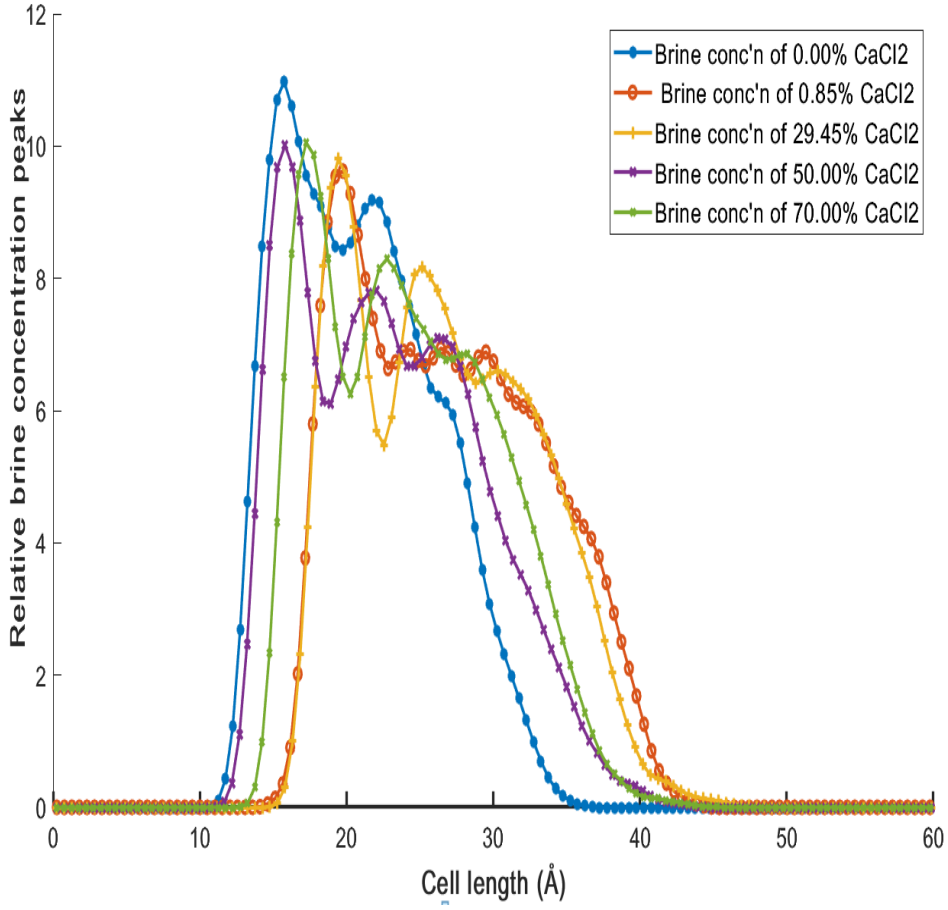

Figure 12. Shows snap shots of oil and CaCl2 brine relative concentrations graphs on quartz surface @ 300K by molecular dynamic (MD) simulation

From the Figure 11 & Figure 12. The relative concentration distribution functions for CaCl2 and NaCl at different concentrations were studied. Unlike for radial distribution functions that measure the probabilities in finding another particle at a distance r from a specific particle, the relative concentration distribution function of brines measures the distribution of brine concentration along Z-direction. The peak value coordinate of the relative concentration distribution function represents the distance of the brine to the quartz interface as a result of the forces acting on the brine ions and vary with concentration[49], [50].

The smaller the z coordinate peak value is, the closer the brine is to the quartz interface, suggesting the stronger the interaction force. From Figure 11: 70% NaCl>0.85% NaCl >50% NaCl >29.45% NaCl while for Figure 12, 0.85% CaCl2 >29.45% CaCl2 >70.0% CaCl2 >50.0% CaCl2 which are attributed to the electrical double-layer expansion, Charge intensity and concentration. Concentrated and highly charged brine ions are attracted close to the interface and adsorb to the electrically negatively charged water−oil interface forming a diffuse ionic layer. While in the absence of salts, the polar components in the oil such as asphaltenes and resins adsorb onto the interface due to their polarity. However, with low brine concentration's diffuse layer is very broad, so the screening is stronger and the polar components of the oil (asphaltenes and resins) are adsorbed and organized at the interface by electrostatic attractions. In Figures 11 &12, the ions in solution move continuously move away from the rock surface with electrostatically attracted oil molecules. The opposite charged particles are attracted from the quartz surface while similar charges are repelled from the surface resulting in concentration difference between brine and the oil molecules. The relative oil concentrations profiles increase with low brine concentrations from 70% < 0.85% <50 % <29.45% for Ca^{2+} and 0% <70% 50% <50 % <29.45% for NaCl. This is due to high ionic charge on the molecules and thus are strongly attracted to the rock surface resulting in less mobility compared to low salinity brines with less attraction and more mobile. This creates an electrical double layer expansion and hence increased disjoining pressure. Similarly, an ionic atmosphere is created where ions are attracted with less independently motion. According to the Debye-Huckel theory of strong electrolyte solution, the concentration can directly reflect the degree of freedom of ion movement in the solution. For very dilute solution, ions are far apart from each other unlike for concentrated solution whose ions are restrained by electrostatic attraction and repulsion of the counter ions. Furthermore, in concentrated solutions, ionic atmosphere association is experienced for positive and negative ions creating a disparity among relative concentrations graphs for different brine solutions and

oil molecules.

3.4 Effect of Brine-Surfactant ions on Oil Detachment from the pore surface

The dynamic motion of oil between quartz surface and brine was found to provide useful insights about fluids motion and interaction between atoms. It was found that fluids motion was strongly dependant on intermolecular forces which comprised primarily hinged on van der Waals, electrical and structural forces as stated in the equation below.

$$\Pi_{Total} = \Pi_{Vdw} + \Pi_{elec} + \Pi_{stru} \quad (6)$$

Where Π_{Total} total disjoining pressure, Π_{Vdw} Van der Waals forces which are negatively charged, Π_{elec} electrostatic forces positively charged and Π_{stru} structural forces . The Van der Waals forces are negative to Crude Oil/ Brine/Rock system while electrostatic and structural the forces are positive [9], [54].The electrical forces play a key role in low salinity brine motion dynamics because the overall total disjoining pressure dictates the wetting scenario.

The disjoining pressure profiles for CaCl2 differs greatly to that measured in NaCl whose profile showed strongly negative disjoining pressures over long-range separation distances beyond 20 nm thus more attractive with increasing CaCl2 concentration and consequently lower relative concentration peaks shown in Figure 12 for CaCl2 Brine compared to Figure 10 for NaCl. Positive disjoining pressures are encountered at short separation distances due to high charged density near the quartz surface. This was reported to decrease from 4.2 nm to 1.2 nm for CaCl2 concentrations from 18 mM to 540 mM[37]. However, when surface wetting components or indigenous acidic species from the crude oil (naphthenic acids) diffuse into aqueous phase resulting into reduction in oil- brine interfacial tension causing the relative concentration shift along the cell as shown for Figures 11&12. Surface tension reduction qualitative measurements confirmed surface tension reduction from 72.8 mN/m for Milli-Q water to 72.0 mN/m at 20 Ċ[37].

3.5 Vander Waals forces

The Van der Waals forces are considered to be negative for Crude Oil/ Brine/Rock systems and the structural and the electrostatic forces are positive forces. The Van der Waals and structural forces have been reported to be the same at all values of water film thickness and molarity[54]. The London-van der Waals force between the two similar materials is usually attractive; therefore, this force is recognized as the strength of the attachment between to solids and is given by the expression below.

$$\Pi_{Vdw}(h) = \frac{-A(15.96h/\lambda + 2)}{12\pi h^3 (1 + 5.32h/\lambda)^2} \quad (7)$$

Where A is the Hamaker constant in an oil/water/solid system, λ is the London wavelength, and h is the distance between the two interfaces. The Hamaker constant for a film system is calculated from the experimentally measured data for two identical bodies in a vacuum. These experimental values agree with the theoretical calculation.

$$A = \frac{3}{4}KT\left(\frac{\varepsilon_1 - \varepsilon_3}{\varepsilon_1 + \varepsilon_3}\right)\left(\frac{\varepsilon_1 - \varepsilon_3}{\varepsilon_2 + \varepsilon_3}\right) + \frac{3H}{4\pi}\int_{V1}^{\infty}\left(\frac{\varepsilon_1(iv) - \varepsilon_3(iv)}{\varepsilon_1(iv) + \varepsilon_3(iv)}\right)\left(\frac{\varepsilon_2(iv) - \varepsilon_3(iv)}{\varepsilon_2(iv) + \varepsilon_3(iv)}\right)dv \quad (8)$$

Where ε_1, ε_2, ε_3 are the static dielectric constants, k is the Boltzmann constant, $\varepsilon_1(iv)$, $\varepsilon_2(iv)$, $\varepsilon_3(iv)$ are the electronic absorption terms, T is the temperature in kelvin. The Hamaker constant for oil/silica in water is approximately 1×10^{-20} J. used Hamaker constants ranging from 0.3 to 0.9×10^{-20} J. In this study, 0.81×10^{-20} J was used as the Hamaker constant, and the London wavelength is assumed to be 100 nm. Lee et al.'s work through small angle neutron scattering, proposed that the film thickness as a function of brine composition and salinity decreases in the order: CaCl2 > NaCl > Na2SO4 and 100 mM > 10 mM[55].This concours with Figure 11&12 where The peaks of NaCl brine are higher than those of CaCl2.

3.6 Electrostatic forces

These forces are as a result of the development of the charges between interacting surfaces which are formed either by dissociation of the surface molecules as in Equation (1), or adsorption of protons onto an uncharged surface and causes adjustment of the electrical double layer. The electrical double layer force is estimated using zeta potentials and is approximated by the equation below[56].

$$\Pi_{elec}(h) = n_b k_B T\left(\frac{2\psi_{r1}\psi_{r2}\cosh(kh) - \psi_{r1}^2 - \psi_{r2}^2}{(\sinh(kh))^2}\right)$$

(9)

here ψ_{r1}, ψ_{r2} are the reduced potential, κ is the reciprocal Debye Huckel double layer length n_b is the ion density in the bulk solution, and k_B is the Boltzmann constant. The Deby-Huckel reciprocal length, κ, is

$$k = \sqrt{\frac{2e^2 z^2 n_b}{\varepsilon_o \varepsilon_r k_B T}}$$

(10)

3.7 Structural forces

The structural forces are short-range interactions at a distance of less than 5 nm compared with the London-van der Waals and electrical double layer forces which are considered long-range interactions. The structural interactions can be calculated from:

$$\Pi_{stru} = A_K \exp\left(-\frac{h}{h_s}\right) \quad (11)$$

Where A_k is the coefficient and h_s is the characteristic decay length for the exponential model. The expansion in the simulation box happens when the total disjoining pressure is positive. This happens when there is significant increase in brine concentrations. For both Sodium chloride and calcium chloride concentration at 6.1w% resulted to a positive disjoining pressure during the MD experiment. However, there was initial negative total Disjoining pressure which was observed as a result of surfactant getting adsorbed on oil-brine interface resulting in decrease in interfacial tension. This phenomenon was reported with other surface-active materials such as Asphaltenes and naphthenic acids in crude oil[57]. This adsorption reached a minimum followed by desorption and ions started getting attracted on the quartz surface, thus rendering the surface oil wet which results in a positive total disjoining pressure[9], [58], [59]. It is worth noting that negative and positive disjoining pressure represent contractive and repulsive forces, respectively[24]. This positive total pressure resulted into fluids motion upwards as shown periodically with electrostatic pull of oil molecules in a simulation cell resulting in oil molecules detached from the quartz surface.

3.8 The effect of salinity on oil layer and quartz surface

The expansion of brine in the simulation cells explain the oil drive mechanisms which occur with time with varying concentrations as shown in Figures 10 &11). As time progresses, the interactions between crude oil and brine increases resulting in transfer of surfactant ions to crude oil-brine interface causing an expansion in brine and thus reduction in contact angle and increase in relative concentration for oil and shown in Figures 10 and 11. It is shown from figure 10 that when salinity increases, contact angle decreases up to a certain salinity limit and then increases. This salinity can be assigned as the optimal salinity for the system and the reduction in contact angle can be attributed to the effect of salt on the interfacial tension between crude oil and aqueous phases. The presence of salts in the aqueous phase has a strong ability to increase the accumulation of the surface-active species present in crude oil at the crude oil−aqueous phase interface, thereby reducing the interfacial tension.

The decrease in NaCl concentration causes expansion of electrical double layer and greater repulsive forces between oil/ brine and rock/brine is created which interfaces with negative electric charges, and thus low-salinity brine creates a water-wet state which is favorable for water improving oil recovery. While the Ca^{2+} in brines can attract negatively charged sites on the rock surface and negatively charged polar groups at oil-water interface by electrostatic attraction which act like a ‘‘bridge” between the rock surface and the oil-water interface, and as a consequence, the rock surface becomes more oil-wet. The higher the salinity of Ca^{2+} is, the more oil-wet the rock becomes, when the absorption of Ca^{2+} on rock surface does not achieve the level of saturation. These suggestions above are in accordance with the zeta potentials of rock/brine and oil/brine interfaces which are shown in Figure 4.

4. Conclusion

(1) The presence of negative charges on quartz surface play an important role in attracting opposite charges to the surface and repelling similar ions from the same surface. This results in creation of total disjoining pressure and brine layer ion adjustment between fluid-fluid and fluid rock interface.

(2) The ion type present in brine has an influence on motion direction are ones responsible for rock wettability adjustment depending on whether adsorbed and desorbed at a given conditions. The surface-active components are attracted on the oil-brine interface and results in decrease in interfacial tension and making the surface more water with reduction in contact angles.

(3) On the contrary, the increase in brine concentrations raise the pH and this increases negative charges on quartz surface which attracts divalent ions (Ca^{2+} ions) to bond with oil molecules resulting in increased oil wetting hydrophobic state.

(4) The dynamic movement of these particles are observed during the molecular dynamic’s simulation. where atoms got attracted on the surface by negative disjoining pressure momentarily, followed by upward motion due to positive disjoining pressure with electrostatic attraction of oil molecules resulting in upward pull and oil detachment.

(5) For the oil molecules on the brine surface, the brine expansion due to the positive disjoining pressure pushes the oil towards the pore center resulting in displacement to the production well.

(6) In the nutshell, the ionic contribution resulting in total pressure adjustment one of the key factors influencing oil detachment and movement in the sandstone rock pores and the dynamic motion can be observed and calculated by molecular dynamics simulation.

Acknowledgements

Financial support: China University of petroleum is gratefully acknowledged.

Reference

[1] D. Zhao *et al.*, "Roles of a mixed hydrophilic/hydrophobic interface in the regulation of nanofiltration membrane fouling in oily produced wastewater treatment: Performance and interfacial thermodynamic mechanisms," *Sep. Purif. Technol.*, vol. 257, no. November 2020, p. 117970, 2021, doi: 10.1016/j.seppur.2020.117970.

[2] E. Pouryousefy, Q. Xie, and A. Saeedi, "Effect of multi-component ions exchange on low salinity EOR: Coupled geochemical simulation study," *Petroleum*, vol. 2, no. 3, pp. 215–224, 2016, doi: 10.1016/j.petlm.2016.05.004.

[3] H. Mahani, A. L. Keya, S. Berg, W. B. Bartels, R. Nasralla, and W. R. Rossen, "Insights into the mechanism of wettability alteration by low-salinity flooding (LSF) in carbonates," *Energy and Fuels*, vol. 29, no. 3, pp. 1352–1367, 2015, doi: 10.1021/ef5023847.

[4] M. E. J. Haagh, I. Siretanu, M. H. G. Duits, and F. Mugele, "Salinity-Dependent Contact Angle Alteration in Oil/Brine/Silicate Systems: the Critical Role of Divalent Cations," *Langmuir*, vol. 33, no. 14, pp. 3349–3357, 2017, doi: 10.1021/acs.langmuir.6b04470.

[5] J. Yang *et al.*, "Wettability Alteration during Low-Salinity Waterflooding and the Relevance of Divalent Ions in This Process," *Energy and Fuels*, vol. 30, no. 1, pp. 72–79, 2016, doi: 10.1021/acs.energyfuels.5b01847.

[6] A. Aladasani, B. Bai, Y. S. Wu, and S. Salehi, "Studying low-salinity waterflooding recovery effects in sandstone reservoirs," *J. Pet. Sci. Eng.*, vol. 120, pp. 39–51, 2014, doi: 10.1016/j.petrol.2014.03.008.

[7] [7] W. B. Bartels, H. Mahani, S. Berg, R. Menezes, J. A. Van Der Hoeven, and A. Fadili, "Low salinity flooding LSF in sandstones at pore scale: Micro-model development and investigation," *Proc. - SPE Annu. Tech. Conf. Exhib.*, vol. 2016-Janua, 2016, doi: 10.2118/181386-ms.

[8] [8] A. N. Awolayo, H. K. Sarma, and L. X. Nghiem, "Brine-dependent recovery processes in carbonate and sandstone petroleum reservoirs: Review of laboratory-field studies, interfacial mechanisms and modeling attempts," *Energies*, vol. 11, no. 11, pp. 1–61, 2018, doi: 10.3390/en11113020.

[9] [9] B. Chandrasekhar and D. Rao, "Application of DLVO Theory to Characterize Spreading in Crude Oil-Brine-Rock Systems," 2007, doi: 10.2523/89425-ms.

[10] J. I. Kilpatrick, S. H. Loh, and S. P. Jarvis, "Directly probing the effects of ions on hydration forces at interfaces," *J. Am. Chem. Soc.*, vol. 135, no. 7, pp. 2628–2634, 2013, doi: 10.1021/ja310255s.

[11] K. S. Sorbie and I. R. Collins, "A proposed pore-scale mechanism for how low salinity waterflooding works," *SPE - DOE Improv. Oil Recover. Symp. Proc.*, vol. 1, pp. 760–777, 2010, doi: 10.2118/129833-ms.

[12] A. S. Ambekar, P. Mattey, and V. V. Buwa, "Pore-resolved two-phase flow in a pseudo-3D porous medium: Measurements and volume-of-fluid simulations," *Chem. Eng. Sci.*, vol. 230, p. 116128, 2021, doi: 10.1016/j.ces.2020.116128.

[13] E. V. Lebedeva and A. Fogden, "Micro-CT and wettability analysis of oil recovery from sand packs and the effect of waterflood salinity and kaolinite," *Energy and Fuels*, vol. 25, no. 12, pp. 5683–5694, 2011, doi: 10.1021/ef201242s.

[14] X. Zhao, M. J. Blunt, and J. Yao, "Pore-scale modeling: Effects of wettability on waterflood oil recovery," *J. Pet. Sci. Eng.*, vol. 71, no. 3–4, pp. 169–178, 2010, doi: 10.1016/j.petrol.2010.01.011.

[15] S. E. Siadatifar, M. Fatemi, and M. Masihi, "Pore scale visualization of fluid-fluid and rock-fluid interactions during low-salinity waterflooding in carbonate and sandstone representing micromodels," *J. Pet. Sci. Eng.*, vol. 198, no. March 2020, p. 108156, 2021, doi: 10.1016/j.petrol.2020.108156.

[16] J. Tang *et al.*, "Molecular Dynamics Simulations of the Oil-Detachment from the Hydroxylated Silica Surface: Effects of Surfactants, Electrostatic Interactions, and Water Flows on the Water Molecular Channel Formation," *J. Phys. Chem. B*, vol. 122, no. 6, pp. 1905–1918, 2018, doi: 10.1021/acs.jpcb.7b09716.

[17] H. Tian and M. Wang, "Molecular dynamics for ion-tuned wettability in oil/brine/rock systems," *AIP Adv.*, vol. 7, no. 12, 2017, doi: 10.1063/1.5003294.

[18] Q. Liu, S. Yuan, H. Yan, and X. Zhao, "Mechanism of oil detachment from a silica surface in aqueous surfactant solutions: Molecular dynamics simulations," *J. Phys. Chem. B*, vol. 116, no. 9, pp. 2867–2875, 2012, doi: 10.1021/jp2118482.

[19] T. R. Underwood and H. C. Greenwell, "The Water-Alkane Interface at Various NaCl Salt Concentrations: A Molecular Dynamics Study of the Readily Available Force Fields," *Sci. Rep.*, vol. 8, no. 1, pp. 1–12, 2018, doi: 10.1038/s41598-017-18633-y.

[20] T. Yu, Q. Li, H. Hu, Y. Tan, and L. Xu, "Molecular dynamics simulation of the interfacial wetting behavior of brine/sandstone with different salinities," *Colloids Surfaces A Physicochem. Eng. Asp.*, vol. 632, no. August 2021, 2022, doi: 10.1016/j.colsurfa.2021.127807.

[21] E. R. Remesal, J. A. Suárez, A. M. Márquez, J. F. Sanz, C. Rincón, and J. Guitián, "Molecular dynamics simulations of the role of salinity and temperature on the hydrocarbon/water interfacial tension," *Theor. Chem. Acc.*, vol. 136, no. 6, pp. 1–6, 2017, doi: 10.1007/s00214-017-2096-9.

[22] M. Samiei Nezhad, D. A. Wood, E. Sadatshojaei, and F. Esmaeilzadeh, "New insight to experimental study of ionic solutions with a non-ionic surfactant on wettability, interfacial tension and micro-model flooding," *Fuel*, vol. 285, no. September 2020, p. 119126, 2021, doi: 10.1016/j.fuel.2020.119126.

[23] B. Wei, J. Ning, J. He, L. Lu, Y. Wang, and L. Sun, "Relation between brine-crude oil-quartz contact angle formed on flat quartz slides and in capillaries with brine composition: Implications for low-salinity waterflooding," *Colloids Surfaces A Physicochem. Eng. Asp.*, vol. 555, no. July, pp. 660–667, 2018, doi: 10.1016/j.colsurfa.2018.07.051.

[24] J. S. Buckley, K. Takamura, and N. R. Morrow, "Influence of electrical surface charges on the wetting properties of crude oils," *SPE Reserv. Eng. (Society Pet. Eng.*, vol. 4, no. 3, 1989, doi: 10.2118/16964-pa.

[25] M. Fattahi Mehraban, S. Ayatollahi, and M. Sharifi, "Role of divalent ions, temperature, and crude oil during water

injection into dolomitic carbonate oil reservoirs," *Oil Gas Sci. Technol. – Rev. d'IFP Energies Nouv.*, vol. 74, p. 36, 2019, doi: 10.2516/ogst/2019003.

[26] J. S. Buckley, C. Bousseau, and Y. Liu, "Wetting alteration by brine and crude oil: From contact angles to cores," *SPE J.*, vol. 1, no. 3, pp. 341–350, 1996, doi: 10.2118/30765-PA.

[27] S. Iglauer, C. H. Pentland, and A. Busch, "CO2 wettability of seal and reservoir rocks and the implications for carbon geo-sequestration," *Water Resour. Res.*, vol. 51, no. 1, pp. 729–774, 2015, doi: 10.1002/2014WR015553.

[28] B. R. Bickmore, J. C. Wheeler, B. Bates, K. L. Nagy, and D. L. Eggett, "Reaction pathways for quartz dissolution determined by statistical and graphical analysis of macroscopic experimental data," *Geochim. Cosmochim. Acta*, vol. 72, no. 18, pp. 4521–4536, 2008, doi: 10.1016/j.gca.2008.07.002.

[29] L. T. Zhuravlev, "The surface chemistry of amorphous silica. Zhuravlev model," *Colloids Surfaces A Physicochem. Eng. Asp.*, vol. 173, no. 1–3, pp. 1–38, 2000, doi: 10.1016/S0927-7757(00)00556-2.

[30] S. Nangia and B. J. Garrison, "Reaction rates and dissolution mechanisms of quartz as a function of pH," *J. Phys. Chem. A*, vol. 112, no. 10, pp. 2027–2033, 2008, doi: 10.1021/jp076243w.

[31] F. A. Rodrigues, P. J. M. Monteiro, and G. Sposito, "Alkali-silica reaction the surface charge density of silica and its effect on expansive pressure," *Cem. Concr. Res.*, vol. 29, no. 4, pp. 527–530, 1999, doi: 10.1016/S0008-8846(98)00220-8.

[32] M. Kobayashi, M. Skarba, P. Galletto, D. Cakara, and M. Borkovec, "Effects of heat treatment on the aggregation and charging of Stöber-type silica," *J. Colloid Interface Sci.*, vol. 292, no. 1, pp. 139–147, 2005, doi: 10.1016/j.jcis.2005.05.093.

[33] P. Li and M. Ishiguro, "Adsorption of anionic surfactant (sodium dodecyl sulfate) on silica," *Soil Sci. Plant Nutr.*, vol. 62, no. 3, pp. 223–229, 2016, doi: 10.1080/00380768.2016.1191969.

[34] Z. Qi, Y. Wang, H. He, D. Li, and X. Xu, "Wettability alteration of the quartz surface in the presence of metal cations," *Energy and Fuels*, vol. 27, no. 12, pp. 7354–7359, 2013, doi: 10.1021/ef401928c.

[35] H. Tian and M. Wang, "Electrokinetic mechanism of wettability alternation at oil-water-rock interface," *Surf. Sci. Rep.*, vol. 72, no. 6, pp. 369–391, 2017, doi: 10.1016/j.surfrep.2018.01.001.

[36] K. Jarrahian, O. Seiedi, M. Sheykhan, M. V. Sefti, and S. Ayatollahi, "Wettability alteration of carbonate rocks by surfactants: A mechanistic study," *Colloids Surfaces A Physicochem. Eng. Asp.*, vol. 410, pp. 1–10, 2012, doi: 10.1016/j.colsurfa.2012.06.007.

[37] S. Tangparitkul *et al.*, "Dewetting dynamics of heavy crude oil droplet in low-salinity fluids at elevated pressures and temperatures," *J. Colloid Interface Sci.*, vol. 596, pp. 420–430, 2021, doi: 10.1016/j.jcis.2021.03.130.

[38] A. A. da Costa *et al.*, "The influence of rock composition and pH on reservoir wettability for low salinity water-CO2 EOR applications in Brazilian reservoirs," *Proc. - SPE Annu. Tech. Conf. Exhib.*, vol. 2019-Septe, 2019, doi: 10.2118/195982-ms.

[39] P. V. Brady, N. R. Morrow, A. Fogden, V. Deniz, N. Loahardjo, and A. Winoto, "Electrostatics and the low salinity effect in sandstone reservoirs," *Energy and Fuels*, vol. 29, no. 2, pp. 666–677, 2015, doi: 10.1021/ef502474a.

[40] Z. Hua, M. Li, X. Ni, H. Wang, Z. Yang, and M. Lin, "Effect of injection brine composition on wettability and oil recovery in sandstone reservoirs," *Fuel*, vol. 182, pp. 687–695, 2016, doi: 10.1016/j.fuel.2016.06.009.

[41] F. Thomas, D. Dalmazzone, and J. F. Morris, "Contact angle measurements on cyclopentane hydrates," *Chem. Eng. Sci.*, vol. 229, 2021, doi: 10.1016/j.ces.2020.116022.

[42] H. Mahani, S. Berg, D. Ilic, W. B. Bartels, and V. Joekar-Niasar, "Kinetics of low-salinity-flooding effect," *SPE J.*, vol. 20, no. 1, pp. 8–20, 2015, doi: 10.2118/165255-pa.

[43] T. Huhtamäki, X. Tian, J. T. Korhonen, and R. H. A. Ras, "Surface-wetting characterization using contact-angle measurements," *Nat. Protoc.*, vol. 13, no. 7, pp. 1521–1538, 2018, doi: 10.1038/s41596-018-0003-z.

[44] V. Khosravi, S. M. Mahmood, D. Zivar, and H. Sharifigaliuk, "Investigating the applicability of molecular dynamics simulation for estimating the wettability of sandstone hydrocarbon formations," *ACS Omega*, vol. 5, no. 36, pp. 22852–22860, 2020, doi: 10.1021/acsomega.0c02133.

[45] Y. Sun, Y. Li, X. Dong, X. Bu, and J. W. Drelich, "Spreading and adhesion forces for water droplets on methylated glass surfaces," *Colloids Surfaces A Physicochem. Eng. Asp.*, vol. 591, no. November 2019, 2020, doi: 10.1016/j.colsurfa.2020.124562.

[46] T. W. Teklu, W. Alameri, H. Kazemi, R. M. Graves, and A. M. AlSumaiti, "Low salinity water–Surfactant–CO2 EOR," *Petroleum*, vol. 3, no. 3, pp. 309–320, 2017, doi: 10.1016/j.petlm.2017.03.003.

[47] V. M. Starov, S. R. Kostvintsev, V. D. Sobolev, M. G. Velarde, and S. A. Zhdanov, "Spreading of liquid drops over dry porous layers: Complete wetting case," *J. Colloid Interface Sci.*, vol. 252, no. 2, pp. 397–408, 2002, doi: 10.1006/jcis.2002.8450.

[48] A. Mabudi, M. Noaparast, M. Gharabaghi, and V. R. Vasquez, "A molecular dynamics study on the wettability of graphene-based silicon dioxide (glass) surface," *Colloids Surfaces A Physicochem. Eng. Asp.*, vol. 569, no. October 2018, pp. 43–51, 2019, doi: 10.1016/j.colsurfa.2019.02.028.

[49] H. Jia *et al.*, "Mechanism studies on the application of the mixed cationic/anionic surfactant systems to enhance oil recovery," *Fuel*, vol. 258, no. August, p. 116156, 2019, doi: 10.1016/j.fuel.2019.116156.

[50] A. A. Skelton, P. Fenter, J. D. Kubicki, D. J. Wesolowski, and P. T. Cummings, "Simulations of the quartz(10$\bar{1}$1)/water interface: A comparison of classical force fields, Ab initio molecular dynamics, and x-ray reflectivity experiments," *J. Phys. Chem. C*, vol. 115, no. 5, pp. 2076–2088, 2011, doi: 10.1021/jp109446d.

[51] S. Li, Y. Liu, L. Xue, L. Yang, and Z. Yuan, "A molecular insight into the effect of key ions on the detachment of crude oil from calcite surface: Implication for low salinity water flooding in carbonate reservoirs," *J. Pet. Sci. Eng.*, vol. 208, no. PC, p. 109562, 2022, doi:

10.1016/j.petrol.2021.109562.

[52] J. Meng, F. Yin, S. Li, R. Zhong, Z. Sheng, and B. Nie, "Effect of different concentrations of surfactant on the wettability of coal by molecular dynamics simulation," *Int. J. Min. Sci. Technol.*, vol. 29, no. 4, pp. 577–584, 2019, doi: 10.1016/j.ijmst.2019.06.010.

[53] Q. Wei, Y. Wang, W. Chai, Y. Zhang, and X. Chen, "Molecular dynamics simulation and experimental study of the bonding properties of polymer binders in 3D powder printed hydroxyapatite bioceramic bone scaffolds," *Ceram. Int.*, vol. 43, no. 16, pp. 13702–13709, 2017, doi: 10.1016/j.ceramint.2017.07.082.

[54] H. Ding and S. Rahman, "Experimental and theoretical study of wettability alteration during low salinity water flooding-an state of the art review," *Colloids Surfaces A Physicochem. Eng. Asp.*, vol. 520, no. February, pp. 622–639, 2017, doi: 10.1016/j.colsurfa.2017.02.006.

[55] S. Y. Lee *et al.*, "Low salinity oil recovery - Increasing understanding of the underlying mechanisms of double layer expansion," *16th Eur. Symp. Improv. Oil Recover. 2011*, pp. 783–795, 2011.

[56] O. E. Godinez-Brizuela and V. J. Niasar, "Effect of divalent ions on the dynamics of disjoining pressure induced by salinity modification," *J. Mol. Liq.*, vol. 291, p. 111276, 2019, doi: 10.1016/j.molliq.2019.111276.

[57] M. Rücker *et al.*, "Relationship between wetting and capillary pressure in a crude oil/brine/rock system: From nano-scale to core-scale," *J. Colloid Interface Sci.*, vol. 562, pp. 159–169, 2020, doi: 10.1016/j.jcis.2019.11.086.

[58] Q. Xie, A. Saeedi, E. Pooryousefy, and Y. Liu, "Extended DLVO-based estimates of surface force in low salinity water flooding," *J. Mol. Liq.*, vol. 221, pp. 658–665, 2016, doi: 10.1016/j.molliq.2016.06.004.

[59] F. Liu and M. Wang, "Review of low salinity waterflooding mechanisms: Wettability alteration and its impact on oil recovery," *Fuel*, vol. 267, no. September 2019, p. 117112, 2020, doi: 10.1016/j.fuel.2020.117112.